

FEB 13 1981

DATE ISSUED

ORNL
MASTER COPY

OAK RIDGE NATIONAL LABORATORY

OPERATED BY
UNION CARBIDE CORPORATION
NUCLEAR DIVISION



POST OFFICE BOX X
OAK RIDGE, TENNESSEE 37830

SPECIAL DISTRIBUTION

ORNL
CENTRAL FILES NUMBER

ORNL/CF-81/30

800a.09

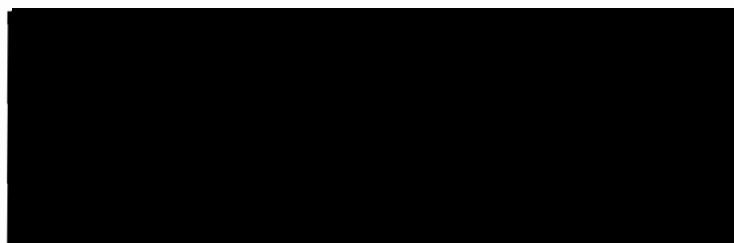
DATE: February 5, 1981

SUBJECT: Technical Highlights of Space and Terrestrial Systems Programs
at Oak Ridge National Laboratory for October 1980

TO: Distribution

FROM: R. H. Cooper

This monthly report is intended to inform the Space and Terrestrial Systems Division, DOE, and their contractors of significant technical highlights of technology and systems support programs in progress at Oak Ridge National Laboratory. A detailed technical presentation of information will be published in topical reports and open literature publications.





CONTENTS

SOLAR-POLAR MISSION MATERIALS SUPPORT	1
Creep Properties of 2219 Aluminum Housing Materials	1
FLIGHT SYSTEMS HARDWARE	10
Iridium Forming Blank Fabrication	10
Iridium Management	12
CBCF-3 Insulation Fabrication	13
MATERIALS TECHNOLOGY SUPPORT	14
Impact Properties of M-Batch DOP-26 Production Sheets	14
Chemistry and Impact Properties of DOP-26 PICS Material	14
Aluminum Segregation to Grain Boundaries in DOP-26	17
Iridium Formability Studies	19
TERRESTRIAL RADIOISOTOPE APPLICATION DEVELOPMENT	20
Cesium-137 Low Solubility Compound	20
Krypton-85 Light Source Development	20
REFERENCES	21
MEETINGS AND PERSONNEL CHANGES	21



SOLAR-POLAR MISSION MATERIALS SUPPORT

(Activity AE 15 15 20 0, WPAS 02313)

R. L. Heestand

This task provides the fabrication development, characterization, and design verification of the General Purpose Heat Source (GPHS) and Thermoelectric Converter for the 1983 Solar-Polar Space Mission. The scope of this task includes determination of physical properties of GPHS components.

Creep Properties of 2219 Aluminum Housing Materials (J. P. Hammond)

The purpose of this task is to develop creep design curves on the 2219-T6 aluminum forging and to aid GE, Valley Forge, in the design of the shell component of the RTG generator. The essential requirement of the shell will be to firmly retain the RTG generator under elastic stress during ground tests and storage in air (condition II), and subsequent flight in vacuum (condition I).

Test specimens were provided from the end cropping of the 2219-T6 forging from which the shell will be fabricated and General Electric, Valley Forge, communicated an agreed-on creep test matrix given in Table 1. The creep test matrix calls for two proof tests to evaluate the magnitude of creep strain under the worst stress-temperature situations envisioned for the shell during the 10,000 h at 270°C flight in space (Test I, Table 1) and the combined ground test of 270°C followed by 10,000 h storage at 177°C (Test II), respectively. To enable assessments of plastic strain in the shell component, design curves establishing the stress-time relationships for 0.2 and 0.1% creep at 260 and 177°C are being determined. Because it is expected that design can be made to preclude a large share of the primary (first stage) creep, the relationships between minimum creep rate and stress at 260 and 177°C will be determined to permit computation of strains that will result from the secondary creep over projected stresses and times of loading.

The results of the creep tests conducted to date are given in Table 2. Total creep strain (ϵ_p) for the time in test (t) are given along with the constant rate of secondary creep (ϵ_m). The latter is only given where it appeared that the steady state may have been attained. Several of the tests failed or were discontinued since last reporting, whereas, the tests on specimens LT 14, T1, and LT 18 were recently initiated. Much of the data on minimum creep rate were revised to reflect the improved accuracy of longer test time.

The computer readout creep curves for proof tests I and II are shown in Figs. 1 and 2, respectively. Indications of the stages of creep response are marked on the graphs along with the computations of ϵ_m . Proof test I, which is a 10,000 h exposure at 270°C under 5 ksi stress (space flight) shows a primary stage of creep from A to B and

secondary creep from B to C for which the constant rate of creep is now $4.5 \times 10^{-7}/h$. The total creep strain through the present 3350 h of testing is 0.22%. However, 6650 h remain to complete the test and computation shows that the specimen will ultimately strain to 0.55% if the present value for $\dot{\epsilon}_m$ is maintained. This total strain is lower than had been earlier computed because with the longer period of testing the minimum creep rate has diminished.

Proof test II which consists of 600 h pretest age at 270°C under 3.5 ksi stress followed by 10,000 h storage at 177°C (on ground), has presently logged 3897 h and has crept a total of 0.119% (Table 1). The region A-B in Fig. 2 represents the creep response during on-ground aging, B-C shows the strain sustained from taking the test from the aging to the storage condition, and C-D-E gives the creep response during the first 3300 h of the storage period. The strain from A to D in Fig. 2 is essentially primary creep and D-E is steady state, for which $\dot{\epsilon}_m$ is now only $4.6 \times 10^{-8}/h$. It is significant to note that the earlier aging (A-B) dissipates the bulk of the primary creep, leaving only about 0.01% (C-D) to be dissipated during the storage stage. Just as the aging stage acted to remove primary creep from the storage phase, so it would appear that the combined age-storage may remove primary creep from the flight stage (condition I) that follows upon the storage (condition II).

We have made up a test to check out this premise; however, we are waiting until a high-accuracy creep frame becomes available before starting it. In performing this experiment, the earlier proof test II will be duplicated up to the point where the early minimum creep rate at 177°C is confirmed and then the conditions of tests will be changed to those of proof test I. Although in the actual transition, probably the temperature and stress would change simultaneously, it will be expedient for us to first reduce the load (from 8.0 to 5.0 ksi) and subsequently alter the temperature (from 177 to 270°C). This test will enable us to assess duplication of test response while establishing the extent to which the primary creep of proof test I is eliminated.

The design curves showing the relationships of stress and time to give 0.1 and 0.2% total creep at 260°C (Test III of Table I are presented in Fig. 3. The tests at 177°C (Test IV) are not sufficiently complete to warrant plotting the data.

The curves in Fig. 3 shown as solid lines through points LT 7, LT 12, and LT 17 are the same as plotted in an earlier report.¹ In the interim, three additional data points were obtained. The dashed curves in Fig. 3 are drawn through sets of three data points of longest test time and represent more conservative estimates of creep response. The

¹Technical Highlights Report, ORNL/CF-80/304, October 7, 1980 – Fig. 3.

latter suggests that for 10,000 h a stress of about 3.2 ksi would be required to give 0.1% creep strain and a stress of 4.7 ksi would be required to produce 0.2% creep.

In Fig. 4 data showing the relationship between stress and minimum creep rate are plotted for the tests performed at 260°C. The data point obtained from proof test I at 270°C is included. Because such data plotted on a log-log graph frequently gives a straight line, they are so represented in this figure. Whereas the data points show some scatter, the results are reasonably good considering that the test specimens were taken from a quenched and artificially aged forging of such large size. By extrapolation to lower test stresses, these results suggest the following. At 260°C a stress of 4.5 ksi would be required to produce 0.2% strain by secondary creep and a stress of 3.6 ksi to give 0.1 strain.

Future creep testing will be aimed at gathering data to lend higher accuracy to the time - total creep and stress - minimum creep rate relationships at 260°C. Additional tests will be started at 177°C.

Table 1. Al 2219-T6 Alloy Creep Test Matrix

Test	Pretest Age	Test Temp (°C)	Stress (psi)	Time (h)	Orientation ^a
I Proof Test	none	270	5000	10,000	LT
II Proof Test	600 h @ 270°C 3500 psi	177	8000	10,000	LT
III Design Data	none	260	TBD(0.2% Creep) ^b	10,000	LT
IV Design Data	none	177	TBD(0.2% Creep) ^b	10,000	LT

^aLT = long transverse.

^bTo be determined.

Table 2. Creep Tests^a on 2219-T6 Forging

Test	Specimen No. ^b	Temp (°C)	Stress (ksi)	Creep, ϵ_p (%)	Time, t (h)	Rate, $\dot{\epsilon}_m$ (%/h)	Status
I, Proof	LT 11	270	5.0	0.220	3350	4.5×10^{-5}	Running
II, Proof	LT 6	270	3.5	0.084	597	^c	----
	LT 6	177	8.0	0.035	3300	4.6×10^{-6}	Running
III, Design	LT 7	260	9.5	0.371	979	2.15×10^{-4}	Discont.
III, Design	LT 12	260	8.2	0.497	2600	1.04×10^{-4}	Failed
III, Design	LT 17	260	7.7	0.870	4061	1.44×10^{-4}	Failed
III, Design	LT 9	260	6.0	0.182	2550	3.6×10^{-5}	Running
III, Design	LT 14	260	5.0	0.031	575	4.2×10^{-5}	Running
III, Design	T 1	260	3.8		425		Running
IV, Design	LT 8	177	7.0	0.151	2658	7.5×10^{-6}	Running
IV, Design	LT 13	177	5.8	0.07	1723	5.0×10^{-6}	Running
IV, Design	LT 18	177	4.8	0.091	576	^c	Running
Preliminary	L 1	260	9.5	0.154	1026	4.6×10^{-5}	Discont.
Preliminary	L 2	177	8.0	0.221	1145	1.5×10^{-5}	Discont.

^aConducted in air.

^bLT and T = long transverse orientation, L = longitudinal.

^cIn primary creep stage.

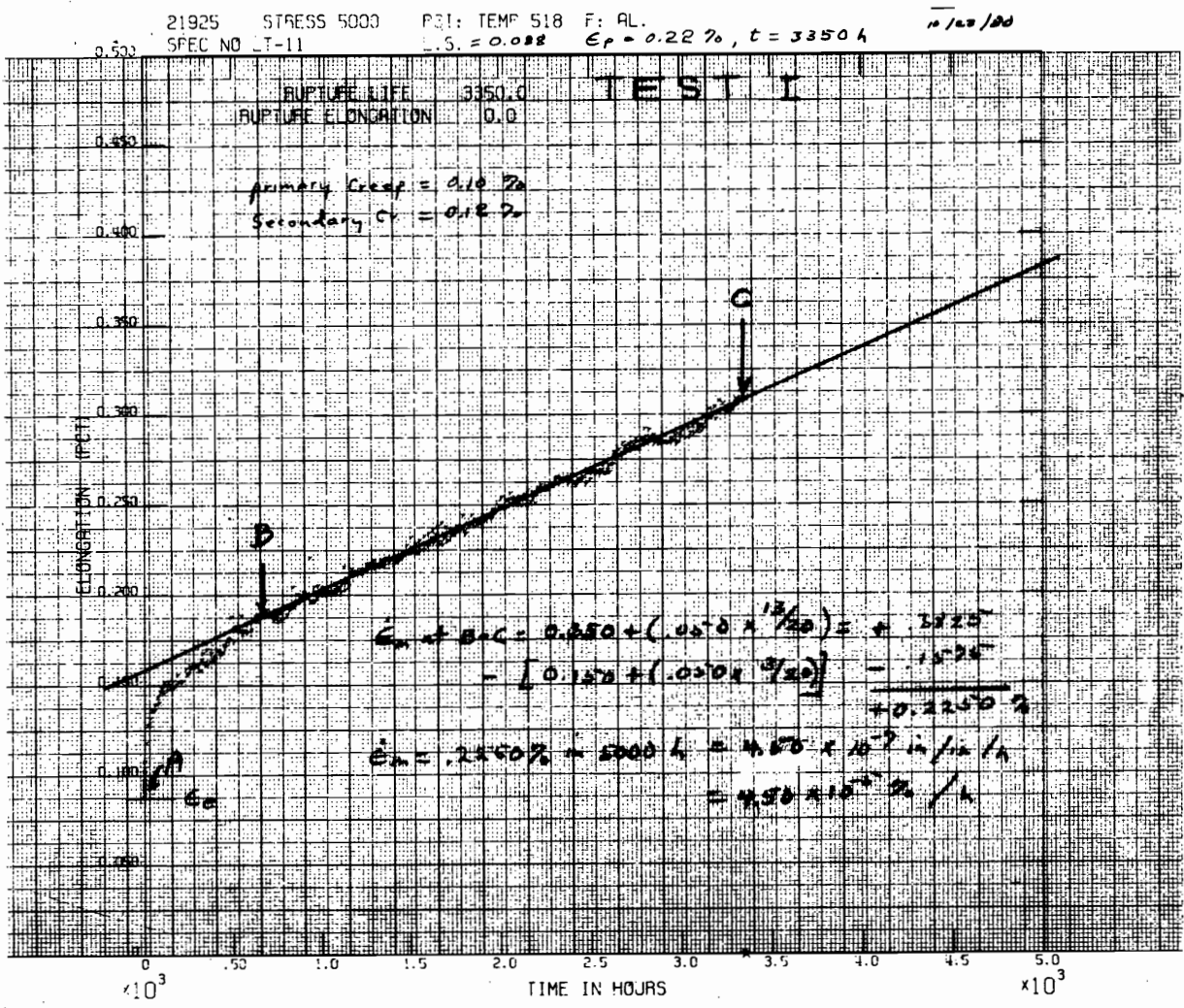


Fig. 1. Creep Curve for Proof Test I (Space Flight).

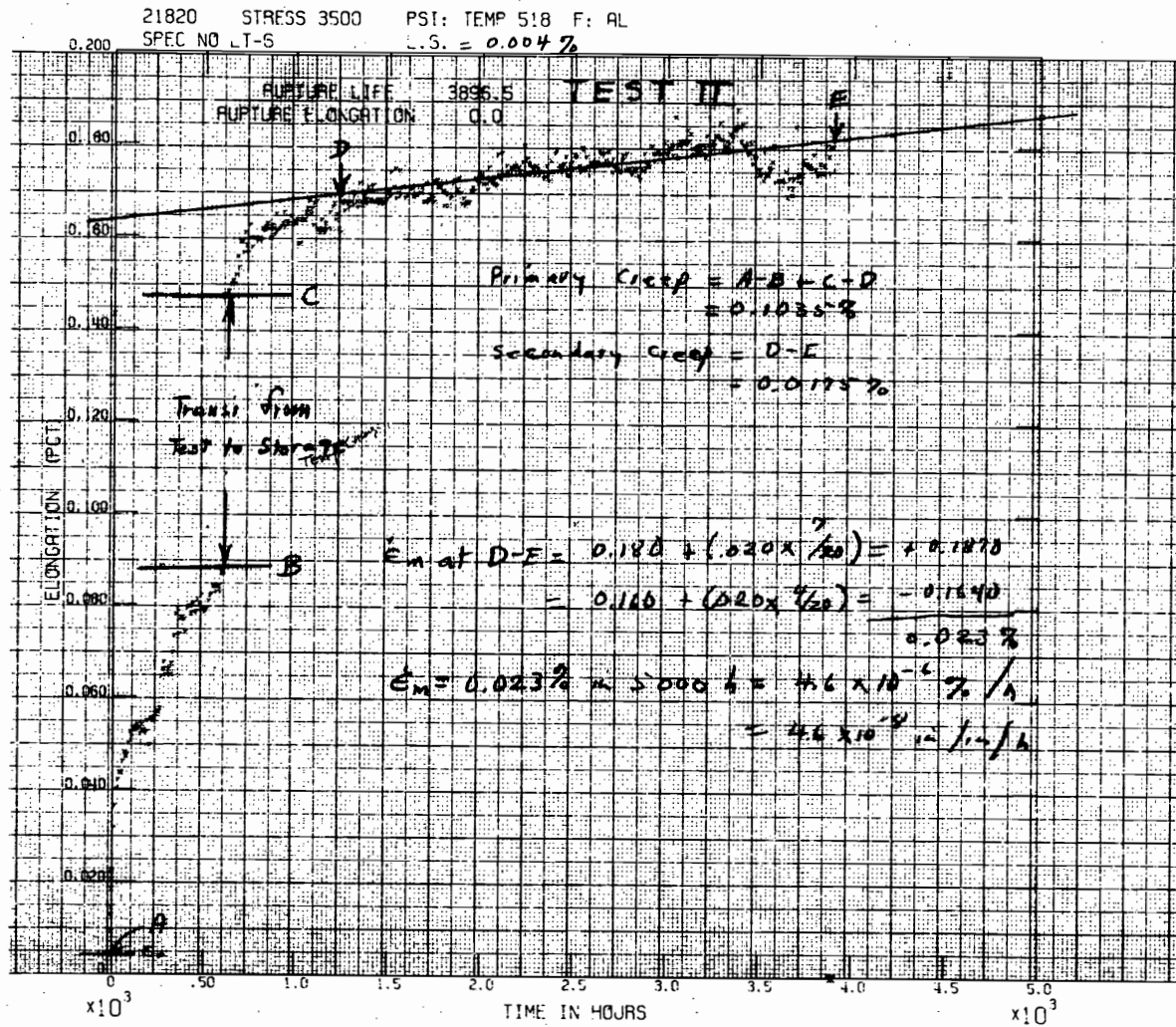


Fig. 2. Creep Curve for Proof Test II [Ground Test (AB) and Storage (CDE)].

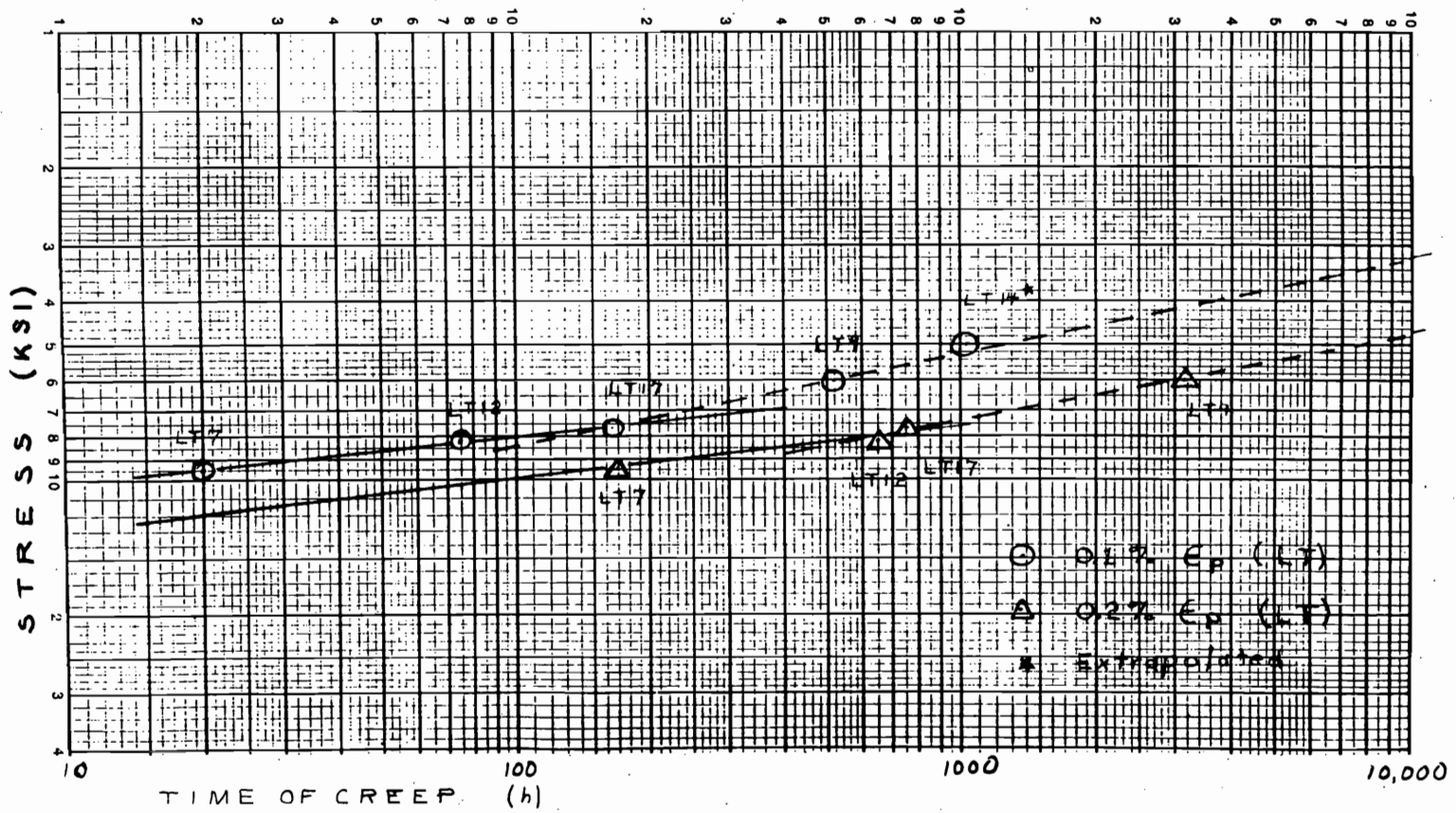


Fig. 3. Design Curves of 2219-T6 Forging Showing Stress-Time Relationship for 0.1 and 0.2% Creep at 260°C.

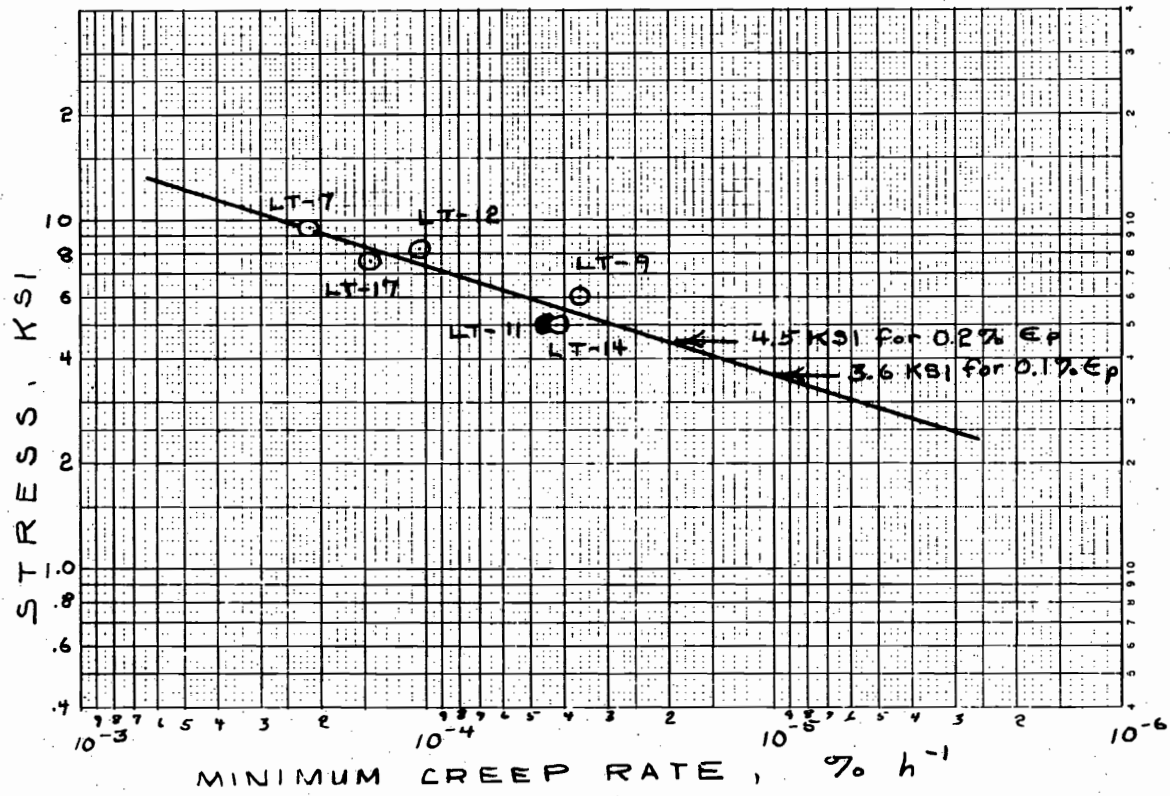


Fig. 4. Graph Showing Stress-Minimum Creep Rate Relationship of 2219-T6 Forging at 260°C.

FLIGHT SYSTEMS HARDWARE

(Activity AE 15 20 00 0 WPAS 01322)

R. L. Beatty
R. L. Heestand

The objective of this task is to supply Mound Facility with flight quality carbon bonded-carbon fiber insulators and iridium hardware components for use in the assembly of isotope heat sources. The major iridium activities are associated with fabrication of iridium alloy forming blanks for isotope fuel capsules and the fabrication of iridium foil for vents, decontamination covers, and weld shields. This task also includes management of the precious metal inventory, iridium refining activities, and coordination of precious metal transfers between other installations.

In addition ORNL is fabricating cylindrical insulator sleeves and end disks from a carbon bonded-carbon fiber material. Techniques to fabricate this light-weight high-temperature insulating material in the components needed for the General Purpose Heat Source were developed at ORNL in FY-1980.

Iridium Forming Blank Fabrication (R. L. Heestand)

Fifty-two forming blanks were received by Mound Facility during the month of October. All discs available for rework had been shipped late in September and plates currently in production are either in rolling or the machine shop. Work was accelerated on the N batch by use of overtime in order to compensate for time lost due to problems with the M batch. Nine ingots were rolled and were in grinding at the end of the month.

Processing of M material with double electron beam melting is continuing. This consists of melting eight times instead of the four times used previously. Analysis of the EB melted material showed a reduction of thorium and aluminum dopants; therefore, dopant levels were adjusted during arc melting. It is anticipated that the remelted M material will be used as flight hardware. A decision was made to double electron beam melt all further material.

The P batch of powder (FY-1981 purchase) arrived late in the month and processing was initiated. The analysis was acceptable and no problems are expected with this material.

A study of the differences between L and M batches has been continued. A comparison of the microhardness of plates made from batches M and N, and the percent of recrystallization was run as a function of annealing temperature. Figure 5 for the microhardness and Fig. 6 for percent recrystallization show essentially no difference in the properties between sheets

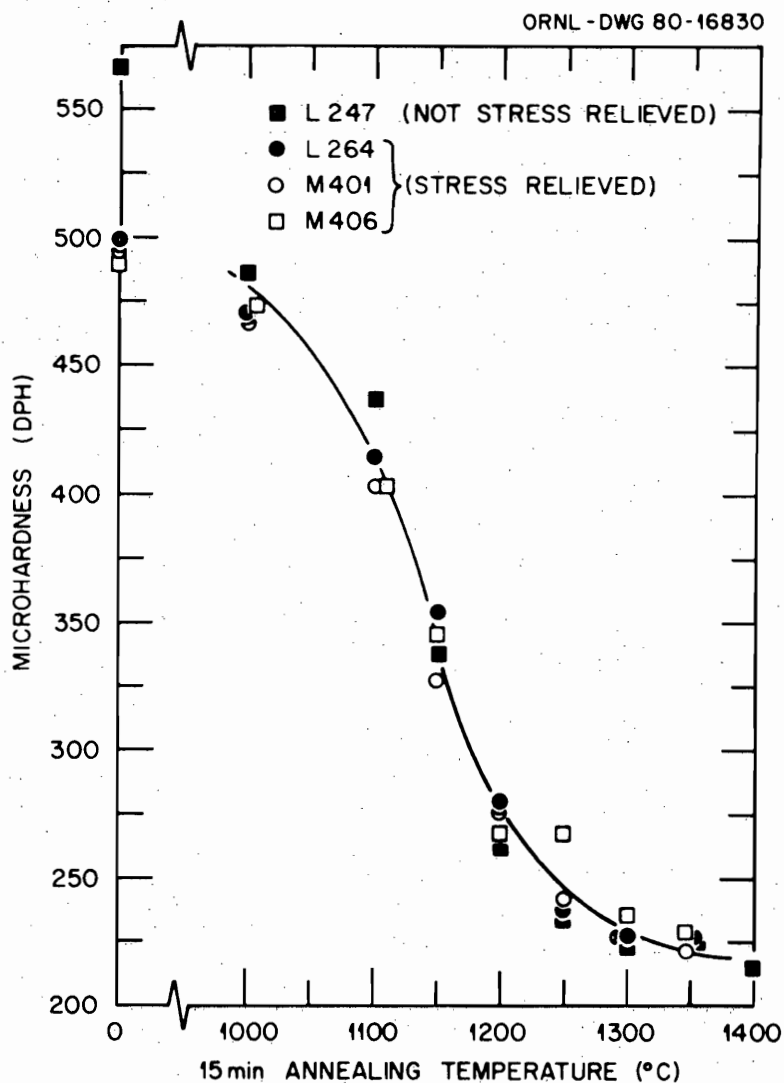


Fig. 5. Comparison of L and M Batch Microhardness as a Function of Temperature.

rolled from the two powder batches. In addition, no difference in chemistry was found with the exception that M appears to have a lower impurity level. These investigations are continuing.

Due to the recent failure of impact test IRG-88, a review of the fabrication history of the discs involved was initiated. It was found that chemistry and metallography was normal and within specification. L242R-2 which failed had the identical fabrication history and was processed with disc L243-5 which was impacted successfully in IRG-87.

ORNL-DWG 80-16829

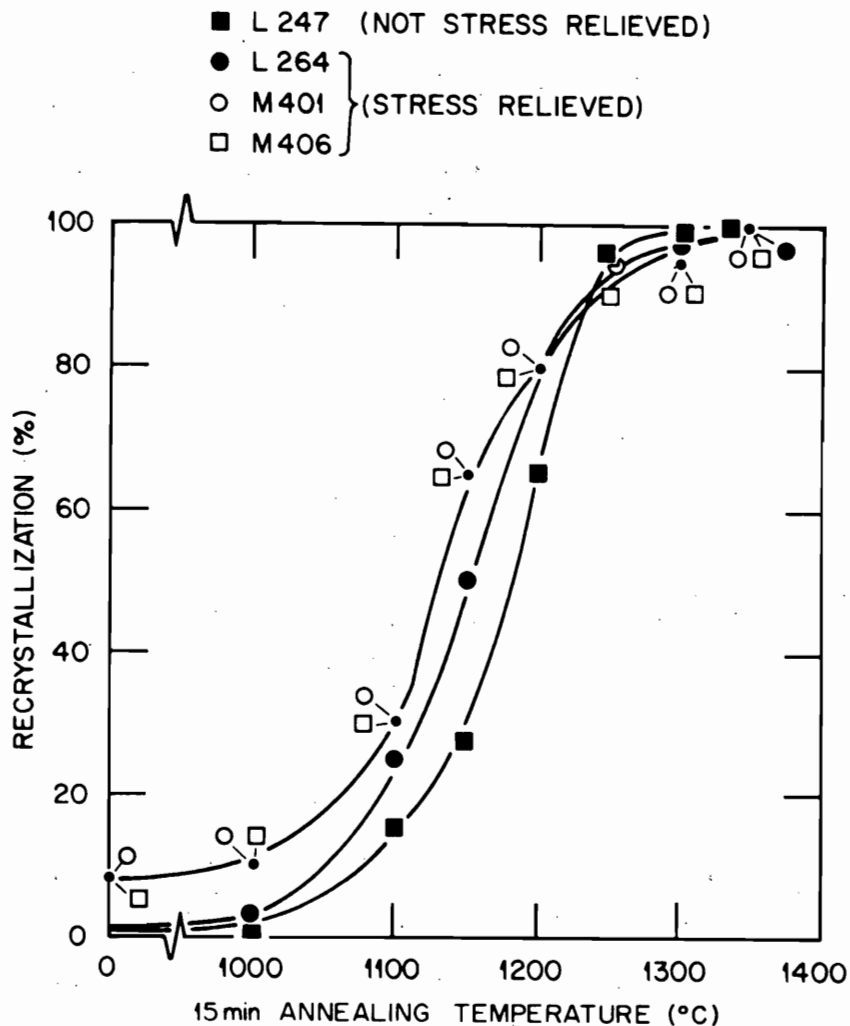


Fig. 6. Comparison of L and M Batch Recrystallization as a Function of Temperature.

Iridium Management (W. O. Graves)

The ORNL Iridium Management Plan was presented at DOE on October 6, 1980. Modifications were made to the financial plan to facilitate the movement of iridium between the contractors primarily by maintaining the total inventory financial plan at ORNL. A meeting was held at ORNL on October 30, 1980, to present the new plan to the contractors.

An iridium refining contract was placed with Engelhard, and approximately 39 kg of scrap was shipped. The assay analysis of this lot is expected by the end of December, and refined material may be available by mid February.

Approximately 12,441 grams of virgin iridium was purchased from Engelhard.

CBCF-3 Insulation Fabrication (J M Robbins)

The procedure for the radiographic inspection of CBCF parts was completed and submitted for approval signatures. All procedures are now in place or have been submitted for approval.

Nine billets from run C-27 were finish machined and inspected. No cracking in these parts was obvious before machining; however, radiographic evaluation after machining revealed linear indications in seven of the nine sleeves. Close visual examination proved these indications were visible to the unaided eye in some cases. Microscopic examination showed definite cracks in three of the sleeves but was not definitive in the others. Scanning electron microscopy analysis on one sleeve showed the linear indication but not definitely. Metallography was done on the same sleeve and indicated that the linear indication was a surface indentation. The cause of these indications in run C-27 has not been determined, and it is not known at this point whether this phenomena is unique to run C-27 or will continue to appear in subsequent runs.

High densities ranging up to about 0.26 Mg/m^3 continue to be a problem. One possible cause of this higher density was identified to the amount of water passed through the molding during fabrication. The speculation was that part of the resin binder might be washed through the filter and lost resulting in lowered density.

Two additional billet molding runs, C-31 and C-32, were made in an effort to meet the November commitment for 16 sleeves. These parts had densities in excess of the presently allowed maximum of 0.232 Mg/m^3 .

Three finished machined sleeves, C-20-2, -3, and -6, were shipped to General Electric Company for use in the Component Engineering Test. Two sleeves, (C-15-2, -4) machined by General Electric Company, were shipped to ORNL for dimensional and radiographic evaluation. These sleeves were subsequently shipped to Los Alamos Scientific Laboratories for their Impact Test No. 3.

MATERIALS TECHNOLOGY SUPPORT

(Activity AE 15 35 00 0, WPAS 01495)

C. T. Liu

The primary objective of this task is to characterize and improve the metallurgical and mechanical properties of noble base alloys, mainly DOP-26 (Ir-0.3% W doped with 60 ppm Th and 50 ppm Al), to meet the requirements of cladding material in radioisotope heat resources for the Galileo and Solar-Polar space missions. The current efforts are concentrated on four areas: (1) to characterize the impact properties of Ir alloys in the temperature range 800–1400°C, (2) to improve the low-temperature impact properties of welds in the DOP-26 alloy, (3) to identify the mechanism and sources that degrade the mechanical and metallurgical properties of doped Ir alloys under heat-source environments, and (4) to develop ductile high-temperature alloys acceptable for future flight missions.

Impact Properties of M-Batch DOP-26 Production Sheets (C. T. Liu)

Impact properties of two DOP-26 sheets M-427 and M-422 produced from normal EB (EB melt for 4 times) and double EB (EB melt for 8 times) melts respectively, were determined at 61 m/s (200 fps) at the temperature from 800 to 1150°C. The tensile specimens prepared from the sheets were annealed for 19 h at 1500°C prior to impact testing. The impact results are presented in Table 3 and plotted in Fig. 7 as a function of test temperature. At temperatures below 1100°C the sheet M-422 produced from the double EB melt shows an impact ductility significantly higher than that of M-427 produced by the normal EB melt. However, both sheets exhibit about the same ductility when tested at 1150°C. Since the double EB melt is expected to remove more impurities in the M-batch Ir powder, the plots in Fig. 7 suggests that DOP-26 alloy becomes insensitive to trace impurities when tested at temperatures above 1100°C.

Chemistry and Impact Properties of DOP-26 PICS Material (C. T. Liu)

Design Verification Tests (DVT) at LANSL showed that the capsule IRG-87 survived while IRG-88 failed on impact at 818–850°C and 58 m/s. In order to identify the reasons for the failure of IRG-88, we have evaluated the chemistry and impact properties of DOP-26 sheet materials which were used to fabricate the PICS (Post Impact Containment Shell) of the two capsules. The results are presented in Table 4 together with the IRG impact data obtained from LANSL. The tensile specimens prepared from the sheets L-243 and L-242R which were the PICS material for IRG-87 and 88 respectively, were heat treated for 19 h at 1500°C prior to impact testing at 820°C. Table 4 indicates that there is no significant difference in the chemistry (in terms of concentration of S, P, Zr, and Th) and impact ductility of the two sheets. Actually,

Table 3. Comparison of Tensile Impact Properties of Two DOP-26 M Sheets Produced From Different Melting Procedures [Impact Velocity: 61 m/s (200 fps)]

Impact Temperature (C°)	Heat Number	Melting Procedure ^a	Impact Elongation (%)
800	M-427	Normal EB melt	5.3
800	M-422	Double EB melt	7.7
980	M-427	Normal EB melt	8.7
980	M-422	Double EB melt	17.2
1050	M-427	Normal EB melt	20.2
1050	M-422	Double EB melt	27.1
1150	M-427	Normal EB melt	33.2
1150	M-422	Double EB melt	31.6

^aNormal EB melt: EB melt for 4 times.
 Double EB melt: EB melt for 8 times.

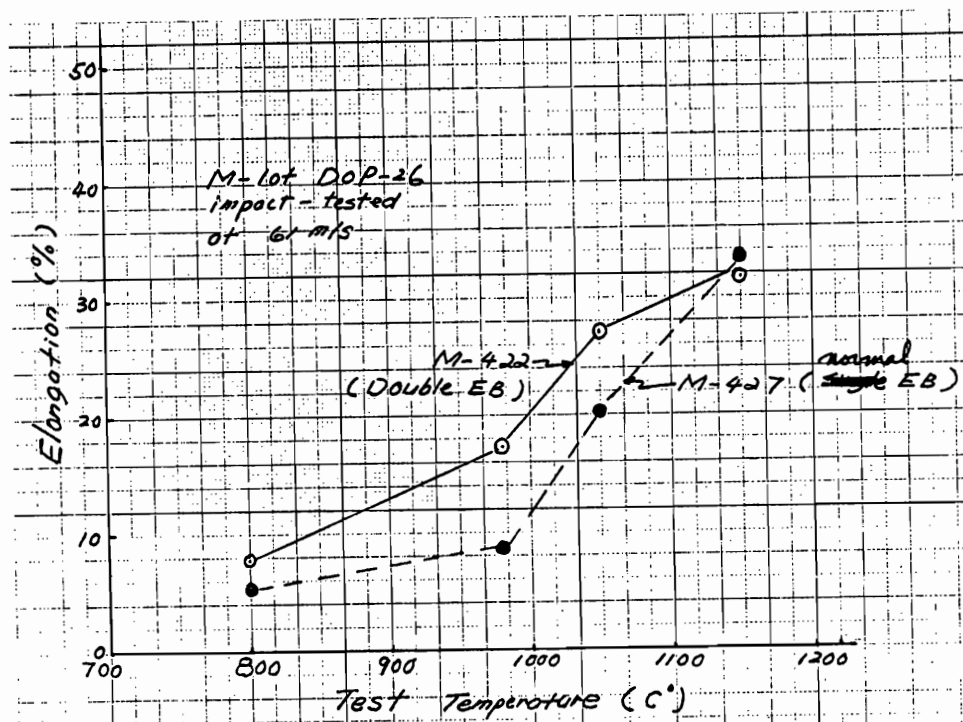


Fig. 7. Plot of Impact Elongation as a Function of Test Temperature for Two M-Batch DOP-26 Sheets Produced From Normal and Double EB Melts.

Table 4. Comparison of Chemistry and Impact Behavior of DOP-26 Sheets L-243 and -242R

<u>IRG Impact</u>		
No.	87	88
Impact Temperature	818°C	850°C
Impact Angle	27°	90°
Strain	10-12%	
Impact Performance	Success	Failure
<u>Sheet Material</u>		
Heat No.	L-243	L-242R
Chemistry (ppm):		
S	1	1
P	<0.1	<0.1
Zr	7	6
Th	45	60
Tensile Impact at 820°C	9.4	11.6

the sheet L-242R had a little better impact ductility. Based on these results, we simply can not attribute the failure of IRG-88 to the properties of the L-242R sheet.

Aluminum Segregation to Grain Boundaries in DOP-26 (C. L. White and R. A. Padgett)

Aluminum is intentionally added to DOP-26 alloys because it is reported to produce a slight improvement in high temperature impact (HTI) ductility beyond that observed with thorium additions alone.¹ While the mechanism of the thorium effect is at least partially understood,* the mechanism for the aluminum effect has remained somewhat of a mystery. Unlike thorium, aluminum has not generally been observed to segregate to grain boundaries in these alloys.⁵

Recent Auger spectra, obtained by W. Moddeman of Mound Facility (MF), indicate significant enrichments of aluminum on an intergranular fracture surface of DOP-26 specimen.⁶ This result is significant in that similar Auger electron spectroscopy (AES) analyses obtained at ORNL have not previously observed such aluminum enrichment at DOP-26 grain boundaries. Figure 8(a) and curve A in Fig. 8(b) show a typical Auger spectrum from an intergranular fracture surface of DOP-26. The relevant portion of the recent MF spectrum, showing the 1346 eV aluminum peak, is traced in Fig. 8(b), curve B for comparison. The difference between the typical ORNL spectrum (curve A) and the MF spectrum (curve B) is clearly evident. Curve C in Fig. 8(b) shows an Auger spectrum from an as-cast Ir + 2% Al alloy.† This spectrum simply verifies the location of the aluminum Auger peak, and gives a rough indication of the relative intensity of aluminum and iridium peaks for this composition.

There is no obvious explanation for the discrepancy between the MF and ORNL results. The bulk aluminum of the MF sample appears to be well within the expected range for DOP-26⁷ and minor increases in bulk aluminum concentration, up to 200 wt ppm, have been found not to result in detectable aluminum concentrations at grain boundaries. Minor variations in thermal history have, likewise, been found not to result in significant aluminum segregation to grain boundaries. Finally, because of the small beam size used in the MF analyses, it is conceivable that the spectrum in curve B, Fig. 8(b) represents, not the overall grain boundary composition, but the surface composition of small

*Thorium is known to segregate strongly to grain boundaries in DOP-26 and other Ir base alloys, as well as form Ir₅Th precipitates which retard grain growth.^{2,3,4} Both the segregation and the grain size control are important to high temperature impact ductility.

†This spectrum is not from an intergranular fracture surface. A small chunk of the as-cast alloy was sputter etched to remove approximately 50 atom layers prior to obtaining the spectrum in curve C, Fig. 8(b).

(aluminum rich) precipitates. While this possibility cannot be completely ruled out at present, two factors tend to discount its likelihood. Firstly, no conscious effort to specifically analyze a precipitate was apparently made, and secondly, qualitatively similar results were apparently observed for approximately six locations on the DOP-26 fracture surface.⁷ Given the small size of the precipitates in DOP-26, and the low area fraction of grain boundaries occupied by them, it seems unlikely that even one, much less six, random analyses would accidentally include a large fraction of these precipitates.

Because of the known effect of aluminum in ductilizing DOP-26 during high temperature impact testing and uncertainty concerning the mechanism for this effect, it is important that the repeatability of the Mound Facility result (and its discrepancy with ORNL results) be verified. The first step in this process should be to repeat these analyses, along with more detailed examination of both grain boundary and precipitate chemistry. If appropriate, similar analyses could then be carried out on the same material at ORNL in an effort to resolve any remaining discrepancies.

Iridium Formability Studies (R. L. Heestand)

Due to defects in cups formed at MF, the previous forming studies conducted at ORNL were reviewed and additional experiments were run. In an experiment to determine minimum forming temperature, a series of discs were formed at temperatures ranging from 430 to 540°C with and without a 950°C - 15 min stress relief. It was determined that fewer defects occurred with the stress relief of 950°C and a forming temperature of 540°. To investigate the effects of higher forming temperature, six additional discs were formed to cups at 580°C following a stress relief of 1000°C for 15 min. Of these six, two had no indications of defects on dye penetrant testing; and only one contained a defect in the radius. Other indications occurred in the side wall; however, no indications are noted on the ID. After rework, five cups showed no defects attributable forming while the one remaining cup contained two pit type indications. These cups were forwarded to MF for further examination. On further inspection at MF, the cups were in tolerance dimensionally but showed additional dye penetrant indications by the more sensitive MF process.

TERRESTRIAL RADIOISOTOPE APPLICATION DEVELOPMENT

(Activity AE 15 35 00 0, WPAS 01367)

F. N. Case, K. W. Haff, and F. J. Schultz

Cesium-137 Low Solubility Compounds

A first draft of the technology transfer document for the ^{137}Cs source compound program entitled, "Preparation and Characterization of Cesium-137 Aluminosilicate Pellets for Radioactive Source Applications" has been completed and submitted for review.

Leaching of the sectioned and unsectioned fully loaded ^{137}Cs aluminosilicate pellets, as well as the tracer level irradiated pellets, is in progress. Leachant samples were collected and the leach rates will be reported next month.

Krypton-85 Light Source Development

Aluminum metal spirals are being tested as a support for light emitting phosphors in the spiral tube light sources. Techniques were developed for coating the metal turning with adhesive and for uniformly coating the adhesive with phosphor powder. Hollow conical frustums suitable for coating with phosphor and insertion into the spiral light tubes are also being fabricated to be tested as phosphor supports in the light sources.

A dark room is being prepared for use in light source intensity measurements. Preparations involve painting all surfaces in the room black and construction of a vertical semicircular rail for use in positioning the photometer probe. A photometer has been ordered and delivery is expected in early January 1981.

The visible and infrared spectrum of the light sources on hand will be measured during the next month.

REFERENCES

1. C. T. Liu, private communication.
2. C. L. White, R. E. Clausing and L. Heatherly, Met. Trans. 10A, 683-691 (1979).
3. D. E. Harasyn and A. C. Schaffhauser, Met. Trans. 10A, 828-830 (1979).
4. C. T. Liu, H. Inouye and A. C. Schaffhauser, Metallurgical and Mechanical Properties of Thorium-Doped Ir-0.3% W Alloys, ORNL-5616 (April 1980).
5. C. L. White, unpublished research, ORNL.
6. W. Moddeman, Report and Presentation to Iridium Task Group Meeting at Mound Facility, October, 1980.
7. W. Moddeman, private communication.

MEETINGS AND PERSONNEL CHANGES

R. H. Cooper and R. L. Heestand attended the GPHS Component Review Meeting held at DOE, Germantown, October 3, 1980.

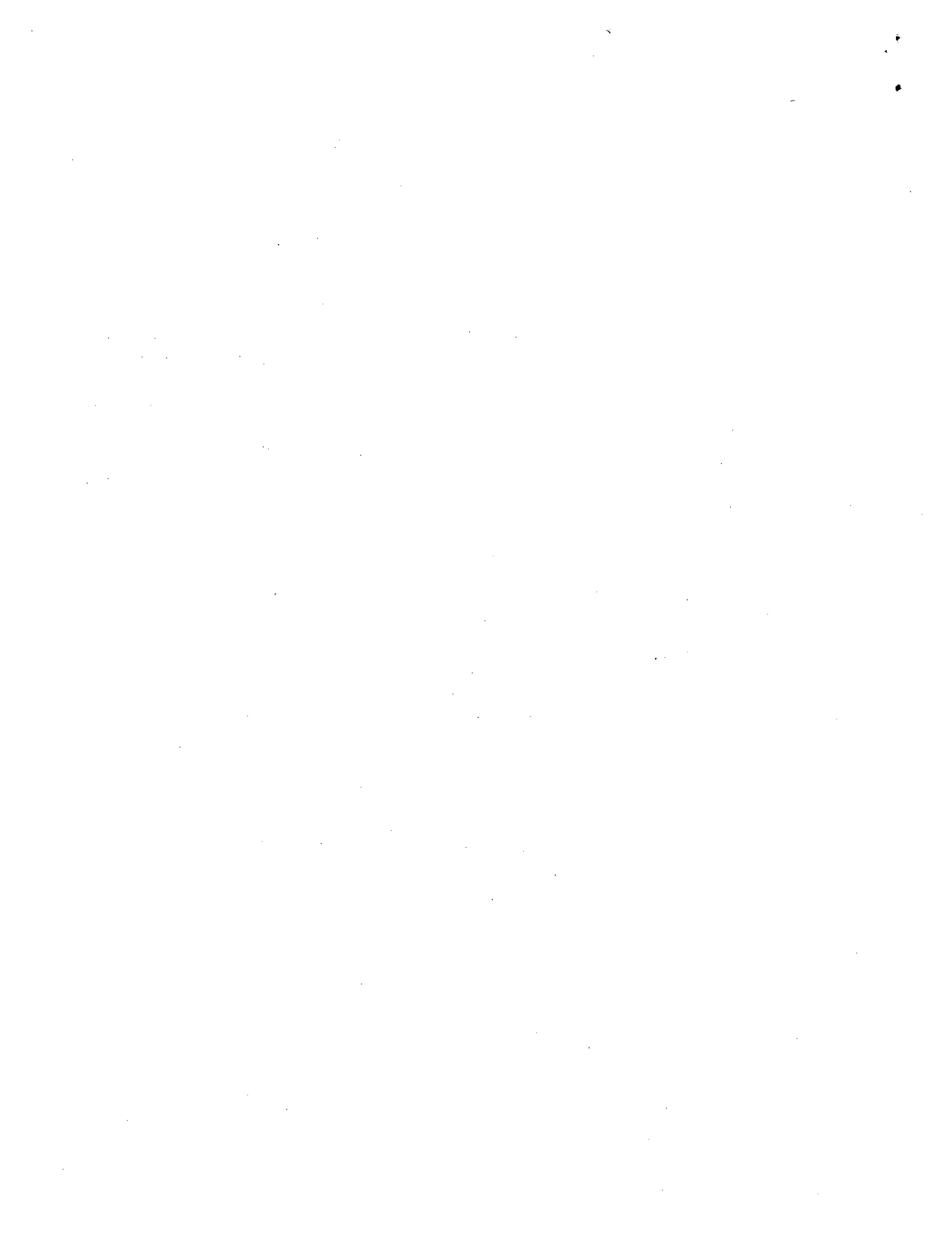
R. H. Cooper and W. O. Graves conducted discussions on the Iridium Management Plan with B. J. Rock at DOE, Germantown, October 6, 1980.

R. H. Cooper, A. C. Schaffhauser, and R. L. Heestand attended an Iridium Production Task Force Meeting held at DOE, Germantown, October 10, 1980.

A. C. Schaffhauser hosted an Iridium Production Task Force Meeting held at ORNL, October 22-23, 1980.

D. E. Harasyn left the program for other employment October 22, 1980.

R. H. Cooper and W. O. Graves held a Contractors Iridium Management Meeting at ORNL, October 30, 1980.



INTERNAL DISTRIBUTION

- | | | | |
|-------|------------------|--------|-----------------------------|
| 1. | E. E. Bloom | 25. | J. W. Koger |
| 2. | C. R. Brinkman | 26. | H. Inouye |
| 3. | J. A. Carter | 27. | E. Lamb |
| 4. | F. N. Case | 28. | C. T. Liu |
| 5-10. | R. H. Cooper | 29. | D. L. McElroy |
| 11. | R. S. Crouse | 30. | C. D. Montgomery |
| 12. | J. E. Cunningham | 31. | T. K. Roche |
| 13. | S. A. David | 32. | A. C. Schaffhauser |
| 14. | J. H. DeVan | 33. | C. S. Sims |
| 15. | R. G. Donnelly | 34. | G. M. Slaughter |
| 16. | W. P. Eatherly | 35. | J. O. Stiegler |
| 17. | J. I. Federer | 36. | V. J. Tennery |
| 18. | G. M. Goodwin | 37. | D. B. Trauger |
| 19. | K. W. Haff | 38. | G. C. Wei |
| 20. | J. P. Hammond | 39. | J. R. Weir, Jr. |
| 21. | W. O. Harms | 40. | C. L. White |
| 22. | R. L. Heestand | 41-45. | Laboratory Records |
| 23. | M. R. Hill | 46. | Laboratory Records, ORNL RC |
| 24. | J. R. Keiser | 47. | ORNL Patent Office |

EXTERNAL DISTRIBUTION

48-59. DOE Space and Terrestrial Systems Division, Washington, DC 20545

G. L. Bennett	J. J. Lombardo
R. C. Brouns	R. B. Morrow
F. M. Dieringer	P. A. O'Riordan
N. Goldenberg	W. C. Remini
J. S. Griffo	B. J. Rock
W. D. Kenney	C. O. Tarr

60-61. DOE Albuquerque Operations Office, P.O. Box 5400,
Albuquerque, NM 87115

D. K. Nowlin
D. Plymale

62-63. DOE Oak Ridge Operations Office, P.O. Box E, Oak Ridge, TN 37830

J. A. Lenhard
J. Pidkowicz

- 64-65. DOE San Francisco Operations Office, 1333 Broadway, Wells Fargo Building, Oakland, CA 94612
L. Lanni
W. L. Von Flue
- 66-67. DOE Savannah River Operations Office, P.O. Box A, Aiken, SC 29801
W. T. Goldston
W. D. Sandberg
68. DOE Dayton Area Office, P.O. Box 66, Miamisburg, OH 45342
H. N. Hill
69. Air Force Weapons Laboratory, Kirtland Air Force Base, DYUS, Albuquerque, NM 87116
Michael Seaton
- 70-71. Battelle Columbus Laboratories, 505 King Ave., Columbus, OH 43201
E. L. Foster
I. M. Grinberg
- 72-73. E. I. du Pont de Nemours, Savannah River Plant, Aiken, SC 29801
R. A. Brownback
W. R. Kanne
- 74-75. E. I. du Pont de Nemours, Savannah River Laboratory, Aiken, SC 29801
R. L. Folger
R. H. Tait
- 76-77. Fairchild Industries, 20301 Century Blvd., Germantown, MD 20767
M. Eck
A. Schock
78. General Atomic Co., P.O. Box 81608, San Diego, CA 92138
N. B. Elsner
- 79-81. General Electric Co., Valley Forge Space Center, P.O. Box 8048, Philadelphia, PA 19101
V. Haley
R. J. Hemler
C. W. Whitmore

- 82-84. Jet Propulsion Laboratory, California Institute of Technology,
4800 Oak Grove Drive, Pasadena, CA 91103
- R. W. Campbell
J. E. Mondt
A. E. Wolfe
85. Johns Hopkins University, Applied Physics Laboratory, Johns
Hopkins Road, Laurel, MD 20810
- J. C. Hagan
- 86-88. Los Alamos National Scientific Laboratory, P.O. Box 1663,
Los Alamos, NM 87545
- S. E. Bronisz
S. S. Hecker
W. J. Maraman
- 89-91. Minnesota Mining and Manufacturing Co., St. Paul, MN 55101
- R. B. Ericson
J. D. Hinderman
W. C. Mitchell
- 92-93. Monsanto Research Corp., P.O. Box 32, Miamisburg, OH 45342
- E. W. Johnson
W. C. Wyder
94. Sundstrand Energy Systems, 4747 Harrison Ave., Rockford, IL 61101
- E. Krueger
- 95-96. Teledyne Energy Systems, 110 W. Timonium Rd., Timonium, MD 21093
- W. J. Barnett
W. E. Osmeyer

